Pharmaceutical Sciences, 2024, 30(2), 215-228
doi:10.34172/PS.2023.29
https://ps.tbzmed.ac.ir/

Research Article

Application of a Deep Eutectic Solvent for the Synthesis of Novel Imidazole-Containing Quinazoline Derivatives as Potent Cytotoxic Agents

Fatemeh Azmian Moghadam[1], Sara Dabirian[2], Amin Ebrahimi Tavani[1], Parisa Alipour[1], Mohammad Mojabi[1], Mehdi Evazalipour[2], Fatemeh Yousefbeyk[3], Saeed Ghasemi[1*]

[1]*Department of Medicinal Chemistry, School of Pharmacy, Guilan University of Medical Sciences, Rasht, Iran.*
[2]*Department of Pharmaceutical Biotechnology, School of Pharmacy, Guilan University of Medical Sciences, Rasht, Iran.*
[3]*Department of Pharmacognosy, School of Pharmacy, Guilan University of Medical Sciences, Rasht, Iran.*

Article Info

Article History:
Received: 9 Sep 2023
Accepted: 11 Dec 2023
ePublished: 15 Jan 2024

Keywords:
-4-anilinoquinazoline
-Cytotoxic activity
-Deep eutectic solvent
-Molecular docking
-Wound healing assay

Abstract

Background: Drugs containing the 4-anilinoquinazolines scaffold play a critical role in cancer treatment by inhibiting protein kinases, especially tyrosine kinases. In this study, a novel series of 4-anilinoquinazoline derivatives were synthesized and evaluated as cytotoxic agents.

Methods: All final compounds were synthesized using two methods, including a conventional approach using potassium iodide and dimethylformamide as well as a green method using a deep eutectic solvent (DES) comprising choline chloride: urea. The cytotoxicity was tested on the A431, HUVEC, and HU02 cell lines. To evaluate the binding pattern of the compounds with EGFR and VEGFR-2, a molecular docking investigation was performed. Finally, the wound healing assay was carried out to assess the potency of compounds in inhibiting cell migration.

Results: The final reaction time was approximately 15-20 min with yields of 60-72% using DES, while the conventional method took 3 to 4 h to complete, with yields between 30% and 42%. Compounds **8k** and **8l** showed better cytotoxicity against both cell lines compared to vandetanib (IC_{50}=0.11 µM and 0.26 µM on A431 and IC_{50}=5.01 µM and 5.24 µM on HUVEC, respectively). Molecular docking studies revealed that compound **8k,** which contained 3-methylaniline at the 4-position of the quinazoline core, showed efficient binding affinity to both EGFR and VEGFR-2. An essential hydrogen bond was formed between quinazoline N1 of **8k** and the **Met796** residue of EGFR with a docking score of -8.76 kcal/mol. The imidazole N3 of **8k** interacted with the **Cyc919** residue of VEGFR-2, forming a hydrogen bond with a docking score of -9.03 kcal/mol. Moreover, compound **8k** exhibited the best inhibitory activity on cell migration and wound healing.

Conclusion: DES significantly improved the time and yield of the final reactions. Compound **8k,** which showed the best cytotoxicity and inhibitory activity on cell migration, could be a suitable candidate for further structural optimization.

Introduction

Malignancies continue to be a serious threat to people worldwide.[1] According to reports from the World Health Organization (WHO), cancer was responsible for approximately 10 million deaths in 2020.[2] The increasing rate of resistance to anticancer drugs, their uncontrollable toxicity, and the lack of selectivity, have made the investigation for new anticancer agents an important area of research.[3] Identifying specific targets, particularly proteins involved in the signal transduction pathways that regulate the proliferation and differentiation of cancer cells, can greatly enhanced the effectiveness of cancer treatment.[4]

Protein kinases are a group of proteins, which catalyze the transfer of a phosphate group from adenosine triphosphate (ATP) to specific residues of a protein, typically serine, threonine, or tyrosine. They have a crucial role in the signal transduction pathway and mediate physiological functions such as cell proliferation, differentiation, migration, and angiogenesis.[5-7] The epidermal growth factor receptor (EGFR) belongs to the ErbB family of receptor tyrosine kinase (RTK) and consists of four closely associated members, including ErbB1(EGFR), ErbB2(HER-2/neu), ErbB3(HER-3), and ErbB4(HER-4).[8,9] When a ligand binds

*Corresponding Author: Saeed Ghasemi, E-mail: ghasemi_saeed@yahoo.com & ghasemi_s@gums.ac.ir

to the extracellular domain of EGFR, it leads to receptor dimerization and autophosphorylation. It activates the tyrosine kinase domain, located in the cytoplasmic region, and consequently triggers downstream signaling pathways.[10] Dysregulated EGFR signaling can occur due to upactivation, overexpression, or mutation of EGFR. It can result in tumor growth and metastasis through the activation of various signal transduction routes (Ras/MAPK, PI3K/Akt, and Jak/STAT) and biological processes.[11,12] Therefore, EGFR can be a promising target for cancer cell-specific therapy and the development of new antitumor agents.[13,14]

Moreover, the formation of new blood vessels from pre-existing vasculature, a process known as angiogenesis, is essential for supplying oxygen and nutrients as well as removing waste materials from tumors. This event plays a crucial role in tumorigenesis and metastasis.[15,16]

Vascular endothelial growth factors (VEGFs) and their receptors (VEGFRs) are vital regulators of both physiological and pathological angiogenesis. The binding of VEGF to VEGFR-2 is the critical pathway that activates angiogenesis. Similar to EGFR, when the dimeric VEGFs bind to the monomeric VEGFR-2, it causes dimerization and activation of the receptor.[2] The activation of vascular endothelial growth factor receptor (VEGFR-2/KDR) can mediate a series of signaling cascade pathways, leading to downstream signal transduction, biological responses, and pathological mechanisms in angiogenesis. These include an increase in vascular permeability, proliferation, and metastasis of cancerous cells.[17,18] Therefore, inhibiting VEGFR-2 activation is an essential target for blocking angiogenesis and cancer chemotherapy.[18,19] EGFR and VEGFR-2, which have common downstream signaling pathways and functional relationships, can be involved in the development of several types of malignancies. Furthermore, blocking EGFR leads to a decline in VEGF expression, which plays a primary role as an inducer of tumor angiogenesis. Also, the inhibition of VEGFR-2 enhances the anticancer activity of EGFR inhibitors.[10,11,20] Consequently, simultaneous inhibition of these signaling pathways can be considered a valuable technique for cancer therapy.[21]

Quinazoline derivatives, which have numerous biological activities, especially as EGFR and VEGFR-2 inhibitors, have attracted a great deal of attention in recent years.[22] The 4-Anilinoquinazoline core has been used in vandetanib (Caprelsa®) as an EGFR/VEGFR-2 dual inhibitor and has received FDA approval for the chemotherapy of different malignancies (Figure 1).[23,24]

This scaffold can interact with the adenosine triphosphate (ATP) binding site of tyrosine kinase domains of both receptors, inhibiting their tyrosine kinase activity.[25-27] The structure-activity relationship (SAR) study of the 4-anilinquinazoline nucleus revealed that small groups, such as fluorine and hydrogen at the ortho position, are more favorable. Lipophilic groups like chlorine, bromine, and ethyl are more acceptable at meta and para positions.

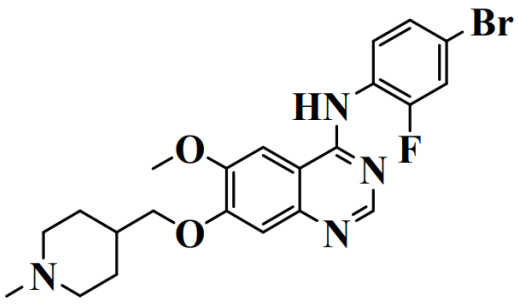

Figure 1. Structures of vandetanib as EGFR/VEGFR-2 tyrosine kinase inhibitor.

Substituents at the C-6 position of the quinazoline core are limited, and the methoxy group is the preferred group in this position. Compounds with various substituents, including neutral and basic groups, as well as nitrogen containing heterocycles at the C-7 position of the quinazoline scaffold, exhibited potent *in vitro* and *in vivo* tyrosine kinase inhibitory activity on EGFR and VEGFR-2 tyrosine kinases.[27-30]

Solvents play a critical role in organic reactions and are a key component of green chemistry. It is important to use solvents that are safe, non-toxic, and biodegradable to protect the environment and humans from the devastating effects of organic solvents. One way to address the environmental issues associated with organic solvents is to replace them with ionic liquids. Ionic liquids have many advantages, such as very low vapor pressure, low flammability, high thermal stability, and the ability to be recycled. However, they are expensive and hard to prepare.[31,32] A new generation of ionic liquids called deep eutectic solvents (DESs) was first reported by Abbott *et al.*[33] in 2003. DESs are formed by mixing two or more solid components and remain liquid form at room temperature. They have unique characteristics that make them attractive substitutes for traditional ionic liquids, including their low cost, biodegradability, sustainability, and the availability of their starting materials.[34-36] They have potential applications in various fields of study such as biochemistry, chemical synthesis, and separation. One commonly used amide-based DES is a mixture of ChCl (2-hydroxyethyl-trimethylammonium chloride) and urea in a 1:2 ratio.[37,38]

Nitrogen-containing heterocycles are the main structural components of drugs in the market. Among these heterocyclic rings, the imidazole ring is found in a wide range of biologically active compounds. The imidazole structure possesses valuable characteristics, including high polarity and its ability to act as a hydrogen bond acceptor. These features make it a promising candidate for interacting with various sites on biological macromolecules. There have been numerous reports on the anticancer activity of imidazole-containing compounds. These derivatives exert their activities by modulating several targets, including tyrosine and serine-threonine kinases, microtubules, p53-Murine Double Minute 2 (MDM2) protein, histone

deacetylases, G-quadruplexes, and poly (ADP-ribose) polymerase (PARP).[39]

In this research, we synthesized 4-anilinoquinazoline compounds bearing imidazole at the C-7 positions of the quinazoline core based on the structure of vandetanib. Two methods were used, including a conventional method using potassium iodide and dimethylformamide, and a green technique using a DES made of choline chloride:urea. To assess the antiproliferation activity of the synthesized compounds, we conducted the MTT assays on three cell lines, including the human epidermoid carcinoma cell line (A431), which overexpresses EGFR, the human umbilical vein endothelial cell (HUVEC), and healthy human foreskin fibroblast cells (HU02). To further analyze the synthesized agents, we examined their binding mode and docking scores on the crystal structures of the EGFR and VEGFR-2 tyrosine kinase domains through docking studies using AutoDock software. Additionally, the wound healing assay was performed to evaluate the effectiveness of the compounds in inhibiting cell migration.

Methods

Chemicals and materials

All chemicals (reagents and solvents) were obtained from Merck (Darmstadt, Germany) and Sigma Aldrich (St. Louis, MO, USA) and used without any purification. The A431 and Hu02 cell lines were purchased from the Iranian Biological Resource Center (IBRC) in Karaj, Iran. The HUVEC cell line was obtained from the national cell bank of Pasteur Institute in Tehran, Iran. Uncorrected melting points were measured using an Electrothermal IA9100 digital melting point apparatus from Staffordshire, UK. Infrared (IR) spectra in the wavenumber range of 4000–400 cm^{-1} were obtained using a Perkin-Elmer Spectrum Two FT-IR spectrometer equipped with universal attenuated total reflectance (UATR). ^{1}HNMR and ^{13}CNMR spectra were recorded using a Bruker FT-500 MHz spectrometer in DMSO-*d6*. Chemical shifts (δ) were reported in parts per million (ppm) and referenced to Tetramethylsilane (TMS) as an internal standard. Mass (MS) spectra were obtained using an Agilent 5973 mass spectrometer with ionization energy of 70 electron volts (eV). Elemental analysis, with a precision of ±0.5% of the calculated values, was performed using a Perkin Elmer 2400 automatic elemental analyzer. The progress of all reactions was monitored by analytical thin layer chromatography (TLC) using TLC Silica gel 60 F_{254} Glass TLC plate, Merck Millipore in Darmstadt, Germany. Purification of synthesized compounds was carried out by column chromatography on Merck silica gel 60 with particle size of 0.06–0.20 mm.

Chemistry

The compounds **1-6** and **7a-l** were synthesized using previously reported techniques.[7,40-48] In brief, the methyl ester of vanillic acid was synthesized (compound **1**) through reacting of vanillic acid with thionyl chloride and methanol. Compound **1** then reacted with 1-bromo-2-chloroethane in the presence of potassium carbonate (K_2CO_3) and tetrabutylammonium bromide (TBAB) to yield compound **2**. Nitration of compound **2** was carried out using sulfuric acid and nitric acid, resulting in compound **3**. Compound **3** was reduced to compound **4** using powdered iron and ammonium chloride. The quinazoline ring was then closed by reacting compound **4** with formamidine acetate and ethanol, producing compound **5**. Chlorination of compound **5** was performed using oxalyl chloride to obtain compound **6**. Coupling compound **6** with appropriate substituted aniline rings yielded the desired compounds **7a-7l**. The synthesis of a deep eutectic reagent was performed using a previously reported technique.[32] Choline chloride and urea were mixed in a molar ratio of 1:2 and heated at 80 °C for 30 min to form the eutectic solvent (ChCl:urea). The liquid was then cooled to room temperature and used for the synthesis of the final compounds without any purification.[49]

General procedure for the synthesis of 8a-8l by conventional method

A mixture of 0.26 mmol of compounds **7a-7l**, 10 mg of potassium iodide, 2 mL of DMF, and 19.5 mg (0.286 mmol) of imidazole was refluxed for 2 h. The mixture was then cooled to ambient temperature before being quenched by crushed ice. The reaction mixture was extracted three times with 5 mL of chloroform each time. The collected chloroform was washed three times with 5 mL of saturated $NaHCO_3$ and 5 mL of brine. The organic layer was dried with anhydrous sodium sulfate (Na_2SO_4) and evaporated under vacuum. The final synthesized compounds were purified using column chromatography filled with silica gel. A solution of ethyl acetate in hexane (4 : 6, v : v) was used for the elution of the final product.[43,50,51]

General procedure for the synthesis of 8a-8l by ChCl:urea

A mixture of 0.26 mmol of compounds **7a-7l** and imidazole (0.286 mmol, 19.5 mg) was added to ChCl:urea (5 equiv.) and the reaction mixture was heated at 80°C for 20 min. Then, the reaction mixture was extracted with ethyl acetate (3×5 mL). The ethyl acetate was dried using anhydrous sodium sulfate (Na_2SO_4) and evaporated under reduced pressure. The final synthesized compounds were purified using column chromatography filled with silica gel. A solution of ethyl acetate in hexane (4 : 6, v : v) was used to elute the final product.

*7-(2-(1H-imidazol-1-yl)ethoxy)-N-(3-chlorophenyl)-6-methoxyquinazolin-4-amine (**8a**)*

mp=207-208°C; IR (vmax, cm^{-1}): 3400 (NH), 1490 (CH_2O), 1290(CH_3O). ^{1}HNMR (DMSO-*d6*, 500 MHz): δppm 9.57 (s, 1H, H-N aniline),8.53(s, 1H, H2 quinazoline), 8.04 (d, J=5 Hz, 1H, H2 aniline), 7.85(s, 1H, H2 imidazole), 7.82 (d, J=8Hz, 1H, H-6 aniline), 7.72 (s, 1H, H-5 quinazoline), 7.42 (t, J=9Hz, 1H, H-5 aniline), 7.29 (brs, 1H, H-4 imidazole) 7.24 (s, 1H, H-8 quinazoline), 6.91 (brs, 1H , H-5 imidazole), 4.46 (brs , 4H, NCH_2, OCH_2), 3.98 (s,

3H, OCH_3). ^{13}CNMR (DMSO-*d6*, 125 MHz) δppm 157.9, 153.2, 149.6, 147.4, 137.7, 129.9, 128.8, 126.8, 123.6, 120.4, 116.3, 108.7, 107.7, 101.7, 100.2, 97.6, 91.2, 61.4, 57.1, 45.8. MS (ESI): m/z 395.2 $[M]^+$. Anal. Calcd for $C_{20}H_{18}ClN_5O_2$: C, 60.68; H, 4.58; N, 17.69. Found: C, 60.89; H, 4.56; N, 17.72.

*7-(2-(1H-imidazol-1-yl)ethoxy)-N-(3-chloro-4-fluorophenyl)-6-methoxyquinazolin-4-amine (**8b**)*

mp=221-223°C; IR (νmax, cm^{-1}): 3405 (NH), 1450 (CH_2O), 1270 (CH_3O). ^{1}HNMR (DMSO-*d6*, 500 MHz): δppm 9.83 (s, 1H, NH aniline), 8.51 (s, 1H, H-2 quinazoline), 8.18 (d, J=5Hz, 1H, H2 aniline), 7.94 (s, 1H, H2 imidazole), 7.86 (dd, J=8Hz, J=3.5Hz , 1H, H-6 aniline), 7.72 (s, 1H, H-5 quinazoline), 7.44 (t, J=9Hz, 1H, H-5 aniline), 7.30 (brs, 1H, H-4 imidazole), 7.24 (s, 1H, H-8 quinazoline), 6.91 (brs, 1H , H-5 imidazole), 4.46 (brs , 4H, NCH_2CH_2O), 3.99 (s, 3H, OCH_3). ^{13}CNMR (DMSO-*d6*, 125 MHz) δppm 159.9, 159.1, 155.5, 148.5, 147.7, 139.0, 135.4, 127.4, 124.0, 123.2, 122.8, 119.6, 118.2, 115.0, 110.0, 105.8, 92.5, 65.5, 55.0, 50.77. MS (ESI): m/z 413.1 $[M]^+$. Anal. Calcd for $C_{20}H_{17}ClFN_5O_2$: C, 58.05; H, 4.14; N, 16.92. Found: C, 57.90; H, 4.15; N, 16.89.[51]

*7-(2-(1H-imidazol-1-yl)ethoxy)-N-(3-bromophenyl)-6-methoxyquinazolin-4-amine (**8c**)*

mp=255-257°C; IR (νmax, cm^{-1}): 3390 (NH), 1410 (CH_2O), 1250 (CH_3O). ^{1}HNMR (DMSO-*d6*, 500 MHz): δppm 9.62 (s, 1H, NH aniline), 8.54 (s, 1H, H-2 quinazoline), 7.92 (brs, 1H, H-5 quinazoline), 7.88 (brs, 1H, H-2 aniline), 7.74 (s, 1H, H-2 imidazole), 7.63 (d, J=8Hz, 1H, H-4 aniline), 7.43 (d, J=6.5Hz, 1H, H-5 aniline), 7.30 (s, 1H, H-6 aniline), 7.25 (s, 1H, H-8 quinazoline), 6.92 (brs, 2H, H-4,5 imidazole), 4.47 (s, 4H, NCH_2CH_2O), 3.99 (s, 3H, OCH_3). ^{13}CNMR (DMSO-*d6*, 125 MHz) δppm 157.9, 153.2, 149.6, 147.4, 143.1, 137.7, 129.9, 128.8, 126.8, 123.6, 120.4, 116.3, 108.7, 108.7, 101.7, 97.6, 91.2, 61.4, 57.1, 45.9. MS (ESI): m/z 439.2 $[M]^+$. Anal. Calcd for $C_{20}H_{18}BrN_5O_2$: C, 54.56; H, 4.12; N, 15.91. Found: C, 54.74; H, 4.13; N, 15.87.

*7-(2-(1H-imidazol-1-yl)ethoxy)-N-(4-bromo-2-methylphenyl)-6-methoxyquinazolin-4-amine (**8d**)*

mp=230-232°C; IR (νmax, cm^{-1}): 3190 (NH), 1415 (CH_2O), 1215 (CH_3O). ^{1}HNMR (DMSO-*d6*, 500 MHz): δppm 9.45 (s, 1H, NH aniline), 8.49 (s, 1H, H-2 quinazoline), 7.86 (s, 1H, H-5 quinazoline), 7.72 (s, 1H, H-8 quinazoline), 7.53 (s, 1H, H-2 imidazole), 7.42 (d, J=8Hz, 1H, H-6 aniline), 7.29 (s, 1H, H-3 aniline), 7.26 (d, J=8Hz, 1H, H-5 aniline), 7.17 (s, 1H, H-4 imidazole), 6.89 (s, 1H, H-5 imidazole), 4.44 (dd, J=8Hz, J=4Hz, 4H, NCH_2CH_2O), 3.94 (s, 3H, OCH_3), 2.16 (s, 3H, CH_3 aniline).^{13}CNMR (DMSO-*d6*, 125 MHz) δppm 158.8, 156.0, 149.6, 147.9, 144.6, 144.4, 138.3, 138.2, 133.1, 128.0, 124.9, 123.2, 120.3, 117.1, 111.6, 102.7, 94.0, 65.9, 56.1, 52.2, 16.5. MS (ESI): m/z 453.3 $[M]^+$. Anal. Calcd for $C_{21}H_{20}BrN_5O_2$: C, 55.52; H, 4.44; N, 15.42. Found: C, 55.74; H, 4.43; N, 15.46.

*7-(2-(1H-imidazol-1-yl)ethoxy)-N-(3-bromo-4-fluorophenyl)-6-methoxyquinazolin-4-amine (**8e**)*

mp=240-242°C; IR (νmax, cm^{-1}): 3400 (NH), 1420 (CH_2O), 1220 (CH_3O). ^{1}HNMR (DMSO-*d6*, 500 MHz): δppm 10.00 (s, 1H, NH aniline), 8.68 (s, 1H, H-2 quinazoline), 8.46 (s, 1H, H-5 quinazoline), 8.14 (s, 1H, H-8 quinazoline), 8.10 (brs, 1H, H-2 aniline), 7.90 (s, 1H, H-2 imidazole), 7.59 (t, J=8.5Hz, 1H, H-5 aniline), 7.47 (s, 1H, H-4 imidazole), 7.41 (s, 1H, H-4 imidazole), 7.09 (brs, 1H, H-6 aniline), 4.64 (brs , 4H, NCH_2CH_2O) , 4.17 (s, 3H, OCH_3). ^{13}CNMR (DMSO-*d6*, 125 MHz) δppm 163.5, 153.2, 149.6, 147.4, 143.1, 129.9, 128.8, 126.8, 123.6, 120.4, 108.7, 107.7, 101.7, 100.2, 99.0, 97.6, 91.2, 68.5, 57.1, 45.9. MS (ESI): m/z 457.2 $[M]^+$. Anal. Calcd for $C_{20}H_{17}BrFN_5O_2$: C, 52.42; H, 3.74; N, 15.28. Found: C, 52.62; H, 3.75; N, 15.31.

*7-(2-(1H-imidazol-1-yl)ethoxy)-N-(3-(trifluoromethyl)phenyl)-6-methoxyquinazolin-4-amine (**8f**)*

mp=278-280°C; IR (νmax, cm^{-1}): 3408 (NH), 1445 (CH_2O), 1230 (CH_3O). ^{1}HNMR (DMSO-*d6*, 500 MHz): δppm 10.14 (s, 1H, NH aniline), 8.53 (s, 1H, H-2 quinazoline), 8.44 (s, 1H, H-5 quinazoline), 8.33 (s ,1H, H-6 aniline), 8.29 (brs, 1H, H-8 quinazoline), 7.73 (s, 1H, H-2 imidazole), 7.63 (t, J=8.5Hz, 1H, H-5 aniline), 7.43 (s, 1H, H-2 aniline), 7.30 (s, 1H, H-4 imidazole), 7.24 (brs, 1H, H-5 imidazole), 4.46 (brs, 4H, NCH_2CH_2O), 4.01 (s, 3H, OCH_3).^{13}CNMR (DMSO-*d6*, 125 MHz) δppm 156.6, 153.5, 153.1, 149.4,147.3, 140.3, 138.1, 138.2, 129.9, 128.7, 125.9, 120.2, 118.3, 109.8, 108.5, 103.1, 101.2, 100.1, 68.3, 57.0, 45.8. MS (ESI): m/z 429.2 $[M]^+$. Anal. Calcd for $C_{21}H_{18}F_3N_5O_2$: C, 58.74; H, 4.23; N, 16.31. Found: C, 58.80; H, 4.24; N, 16.62.

*3-(7-(2-(1H-imidazol-1-yl)ethoxy)-6-methoxyquinazolin-4-ylamino)benzonitrile (**8g**)*

mp=258-260°C; IR (νmax, cm^{-1}): 3985 (NH), 1432 (CH_2O), 1228 (CH_3O). ^{1}HNMR (DMSO-*d6*, 500 MHz): δppm 9.8 (s, 1H, NH aniline), 8.51 (brs, 2H, H-2,5 quinazoline), 7.95 (s, 1H, H-8quinazoline), 7.92 (d, J=8.5Hz, 1H, H-5 aniline), 7.71 (s, 1H, H-2 imidazole), 7.65 (d, J=8.5Hz, 1H, H-4 aniline), 7.41 (d, J=8.5Hz, 1H, H-6 aniline), 7.28 (s, 1H, H-4 imidazole), 7.23 (s, 1H, H-5 imidazole), 6.90 (s, 1H, H-2 aniline), 4.45 (brs ,4H, NCH_2CH_2O), 3.98 (s, 3H, OCH_3). ^{13}CNMR (DMSO-*d6*, 125 MHz) δppm 156.0, 153.4, 152.5, 149.0, 146.9,143.1, 141.8, 136.9, 131.7, 123.3, 122.26, 122.21, 116.4, 116.2, 108.9, 107.9, 102.3, 91.6, 66.7, 56.5, 47.0. MS (ESI): m/z 423.4 $[M]^+$. Anal. Calcd for $C_{21}H_{18}N_6O_2$: C, 65.27; H, 4.70; N, 21.75. Found: C, 65.15; H, 4.71; N, 21.78.

*7-(2-(1H-imidazol-1-yl)ethoxy)-N-(3-ethylphenyl)-6-methoxyquinazolin-4-amine (**8h**)*

mp=270-272°C; IR (νmax, cm^{-1}): 3376 (NH), 1439 (CH_2O), 1223 (CH_3O). ^{1}HNMR (DMSO-*d6*, 500 MHz): δppm 9.64 (s, 1H, NH aniline), 8.50 (s, 1H, H-2 quinazoline), 8.22 (s, 1H, H-5 quinazoline), 8.08 (brs, 1H, H-8 quinazoline), 7.87 (brs, 2H, H-4,6 aniline), 7.63 (s, 1H, H-2 imidazole), 7.42 (m, 1H, H-5 aniline), 7.24 (s, 1H, H-4 imidazole), 7.12

(s, 1H, H-5 imidazole), 7.24 (brs, 1H , H-2 aniline), 4.52 (brs ,4H, NC$\underline{H}_2$C$\underline{H}_2$O), 3.97 (s, 3H, OCH_3), 2.51 (s, 2H, CH_2), 1.25 (s, 3H, CH_3). ^{13}CNMR (DMSO-*d6*, 125 MHz) δppm 156.0, 153.9, 153.4, 152.5, 149.0, 146.9, 136.9, 123.3, 122.26, 122.21, 116.4, 116.2, 108.9, 107.9, 102.3, 91.6, 66.8, 66.7, 56.5, 47.0, 26.4, 11.3. MS (ESI): m/z 389.1 $[M]^+$. Anal. Calcd for $C_{22}H_{23}N_5O_2$: C, 67.85; H, 5.95; N, 17.98. Found: C, 68.07; H, 5.96; N, 17.95.

*7-(2-(1H-imidazol-1-yl)ethoxy)-N-(3-fluorophenyl)-6-methoxyquinazolin-4-amine (**8i**)*

mp=231-232°C; IR (*ν*max, cm^{-1}): 3490 (NH), 1432 (CH_2O), 1283 (CH_3O). ^{1}HNMR (DMSO-*d6*, 500 MHz): δppm 9.90 (s, 1H, NH aniline), 8.53 (s, 1H, H-2 quinazoline), 8.01 (s, 1H, H-5 quinazoline), 7.94 (d, J=12Hz, 1H, H-6 aniline), 7.94 (d, J=8Hz, 1H, H-4 aniline), 7.72 (d, J=7Hz, 1H, H-2 aniline), 7.69 (s, 1H, H-2 imidazole), 7.41(d, J=7.5Hz, 1H, H-5 aniline), 7.30 (s, 1H, H-8 quinazoline), 7.24 (s, 1H, H-4 imidazole), 6.93 (s, 1H, H-5 imidazole), 4.46 (brs, 4H, NC$\underline{H}_2$C$\underline{H}_2$O), 4.00 (s, 3H, OCH_3). ^{13}CNMR (DMSO-*d6*, 125 MHz) δppm 156.6, 153.4, 153.2, 149.3, 147.3, 140.3, 129.3, 126.7, 125.2, 123.1, 122.1, 109.7, 108.6, 102.9, 101.4, 84.0, 81.0, 68.3, 63.5, 57.02. MS (ESI): m/z 379.6 $[M]^+$. Anal. Calcd for $C_{20}H_{18}FN_5O_2$: C, 63.32; H, 4.78; N, 18.46. Found: C, 63.59; H, 4.77; N, 18.48.

*7-(2-(1H-imidazol-1-yl)ethoxy)-N-(4-bromo-2-fluorophenyl)-6-methoxyquinazolin-4-amine (**8j**)*

mp=240-242°C; IR (*ν*max, cm^{-1}): 3412 (NH), 1426 (CH_2O), 1219 (CH_3O). ^{1}HNMR (DMSO-d6, 500 MHz): δppm 9.81 (s, 1H, NH aniline), 8.51 (s, 1H, H-2 quinazoline), 7.95 (brs, 2H, H-5,8 quinazoline), 7.71 (s, 1H, H-2 imidazole), 7.65 (d, J=8.5Hz, 1H, H-4 imidazole), 7.38 (d, J=8.5Hz, 1H, H-5 imidazole), 7.28 (s, 1H, H-3 aniline), 7.23 (s, 1H ,H-6 aniline), 6.90 (brs, 1H, H-5 aniline), 4.45 (brs, 4H, NC$\underline{H}_2$C$\underline{H}_2$O), 3.98 (s, 3H, OCH_3). ^{13}CNMR (DMSO-d6, 125 MHz) δppm 159.8, 157.5, 150.6, 146.3, 138.2, 138.0, 136.4, 136.1, 128.5, 128.5, 127.4, 125.4, 125.1, 122.1, 119.3, 113.3, 92.7, 62.7, 54.5, 50.0. MS (ESI): m/z 423.4 $[M]^+$. Anal. Calcd for $C_{20}H_{17}BrFN_5O_2$: C, 52.42; H, 3.74; N, 15.28. Found: C, 52.29; H, 3.75; N, 15.31.[51]

*7-(2-(1H-imidazol-1-yl)ethoxy)-6-methoxy-N-m-tolylquinazolin-4-amine (**8k**)*

mp=248-250°C; IR (*ν*max, cm^{-1}): 3300 (NH), 1490 (CH_2O), 1270 (CH_3O). ^{1}HNMR (DMSO-d6, 500 MHz): δppm 9.55 (s, 1H, NH aniline), 8.45 (s, 1H, H-2 quinazoline), 7.96 (s, 1H, H-5 quinazoline), 7.73 (s, 1H, H-6 aniline), 7.67(d, J=8Hz, 1H, H-4 aniline), 7.62 (s, 1H, H-2 imidazole), 7.31 (s, 1H, H-2 aniline), 7.27 (t, J=8Hz, 1H, H-5 aniline), 7.20 (s, 1H, H-4 imidazole), 6.94 (s, 1H, H-5 imidazole), 6.93 (s, 1H, H-8 quinazoline), 4.45 (brs, 4H, NC$\underline{H}_2$C$\underline{H}_2$O), 3.98(s, 3H, OCH_3), 2.34(s, 3H, CH_3 aniline). ^{13}CNMR (DMSO-*d6*, 125 MHz) δppm 159.5, 156.1, 151.5, 148.8, 141.0, 139.0, 135.8, 132.9, 131.6, 127.5, 123.3, 120.6, 114.8, 111.4, 109.8, 107.8, 89.5, 65.0, 56.0, 51.6, 16.5. MS (ESI): m/z 375.2 $[M]^+$. Anal. Calcd for $C_{21}H_{21}N_5O_2$: C, 67.18; H, 5.64; N, 18.65. Found: C, 67.38; H, 5.65; N, 18.70.

*7-(2-(1H-imidazol-1-yl)ethoxy)-N-(3-ethynylphenyl)-6-methoxyquinazolin-4-amine (**8l**)*

mp=238-240°C; IR (*ν*max, cm^{-1}): 3300 (NH), 1482 (CH_2O), 1266 (CH_3O). ^{1}HNMR (DMSO-d6, 500 MHz): δppm 9.73 (s, 1H, NH aniline), 8.50 (s, 1H, H-2 quinazoline), 8.04 (d, J=5Hz, 1H, H-2 aniline), 7.96 (s, 1H, H-2 imidazole), 7.94 (d, J=8Hz, 1H, H-6 aniline), 7.73 (s, 1H, H-C5 quinazoline), 7.40 (t, J=9Hz, 1H, H-C5 aniline), 7.22 (brs, 1H, H-C4 imidazole) 7.24 (s, 1H, H-C8 quinazoline), 6.92 (brs, 1H , H-5 imidazole), 4.46 (brs, 4H, NC$\underline{H}_2$C$\underline{H}_2$O), 4.20 (s, 1H, H-ethynyl), 3.99 (s, 3H, OCH_3). ^{13}CNMR (DMSO-d6, 125 MHz) δppm 156.6, 153.4, 153.2, 149.3, 147.3, 140.3, 129.3, 126.7, 125.2, 123.1, 122.1, 109.7, 108.6, 108.60, 102.9, 101.4, 84.02, 81.01, 68.3, 63.6, 63.5, 57.0. MS (ESI): m/z 385.2 $[M]^+$. Anal. Calcd for $C_{22}H_{19}N_5O_2$: C, 68.56; H, 4.97; N, 18.17. Found: C, 68.63; H, 4.94; N, 18.24.

Antiproliferation assay

The MTT method was used to evaluate the cytotoxicity of synthesized compounds (**8a**-**l**) on the A431 (human epidermoid carcinoma), HUVECs (human umbilical vein endothelial cells), and HU02 (human foreskin fibroblast) cell lines as described in previous studies.[52-54] Cells with a density of 5×10^3 per well were seeded in 96-well plates and incubated under a humidified atmosphere with 5% CO_2 (24 h, 37°C). A solution of various concentrations (1, 2, 5, 10, 20, 50, 100, 200, and 500 µM) of compounds and vandetanib in a medium with 0.1% DMSO was added to the cells. The solvent was used as the negative control. After 72 h of treatment, a solution of 5 mg/mL of MTT in PBS was added to each well. The cells were incubated with MTT for 3 h at 37°C, and then the additional MTT was removed. Formazan crystals in each well were dissolved in 150 µL of DMSO. Finally, the absorbance of the dissolved formazan was measured at 570 nm using a Biotek Epoch™ microplate reader.

Statistical analysis

All tests were conducted in triplicate. The calculation of IC_{50} values (the concentration required for 50% inhibitory activity) was performed using nonlinear regression with the normalized fitted dose-response curve (GraphPad Software., version 5, Inc. San Diego, USA). The results were expressed as mean ± standard deviation (S.D.) in µM.[55]

Molecular docking

Molecular docking studies of the most potent compound (**8k**) and vandetanib were conducted on EGFR and VEGFR-2 using AutoDock 4.2 and AutoDock Tools 1.5.4 (ADT). The x-ray crystallography data of co-crystalized EGFR tyrosine kinase domain with erlotinib (PDB ID: 1M17, resolution of 2.6 Å) and co-crystalized VEGFR-2 kinase domain with a 2,3-dihydro-1,4-benzoxazine inhibitor (PDB ID: 2RL5, resolution of 2.65 Å) were downloaded from the protein data bank (http://www.rcsb.

org) and used for the docking studies. Ligands and water molecules were removed from structures of EGFR and VEGFR-2, and hydrogens and Kollman charges were added. Nonpolar hydrogens were merged accordingly. Chemical structures were constructed and molecular geometries were optimized using HyperChem 8.0 software, employing the molecular mechanics force field (MM+ method) and AM1 as the semi-empirical method. The grid box dimensions were set at 90×90×90 with a grid-point spacing of 0.375 Å. The Lamarckian genetic search algorithm (LGA) was utilized for the conformational search with 100 GA runs conducted for each ligand. Erlotinib and 2,3-dihydro-1,4-benzoxazine as co-crystallized ligands were used to validate the docking technique based on aforementioned method.[40]

Wound healing assay

HUVEC cells were utilized for this experiment. To form a cell monolayer, the HUVEC cells were plated in a 24-well plate containing high glucose DMEM, and incubated for 24 h. A scratch was created in the center of each well using a P200 pipette tip. The wells were then washed and fresh media were added to each well. Next each well was exposed to 0.2 µM of compounds **8b**, **8c**, **8f, 8g, 8k,** and **8l,** and images were captured using a fluorescence microscope. After 24 h of incubation at 37°C in a 5% CO_2 atmosphere, the photographs were taken to evaluate the percentage of cell migration before and after using the synthesized compounds.[55,56]

Results and Discussion

The synthesis of compounds **8a-8l** was demonstrated in Figure 2. Compounds **1-6** and **7a-7l** were synthesized using previously reported methods.[7,22,40,41,43-48,57] The final reaction between compounds 7a-7l and imidazole was conducted using both green and conventional methods.

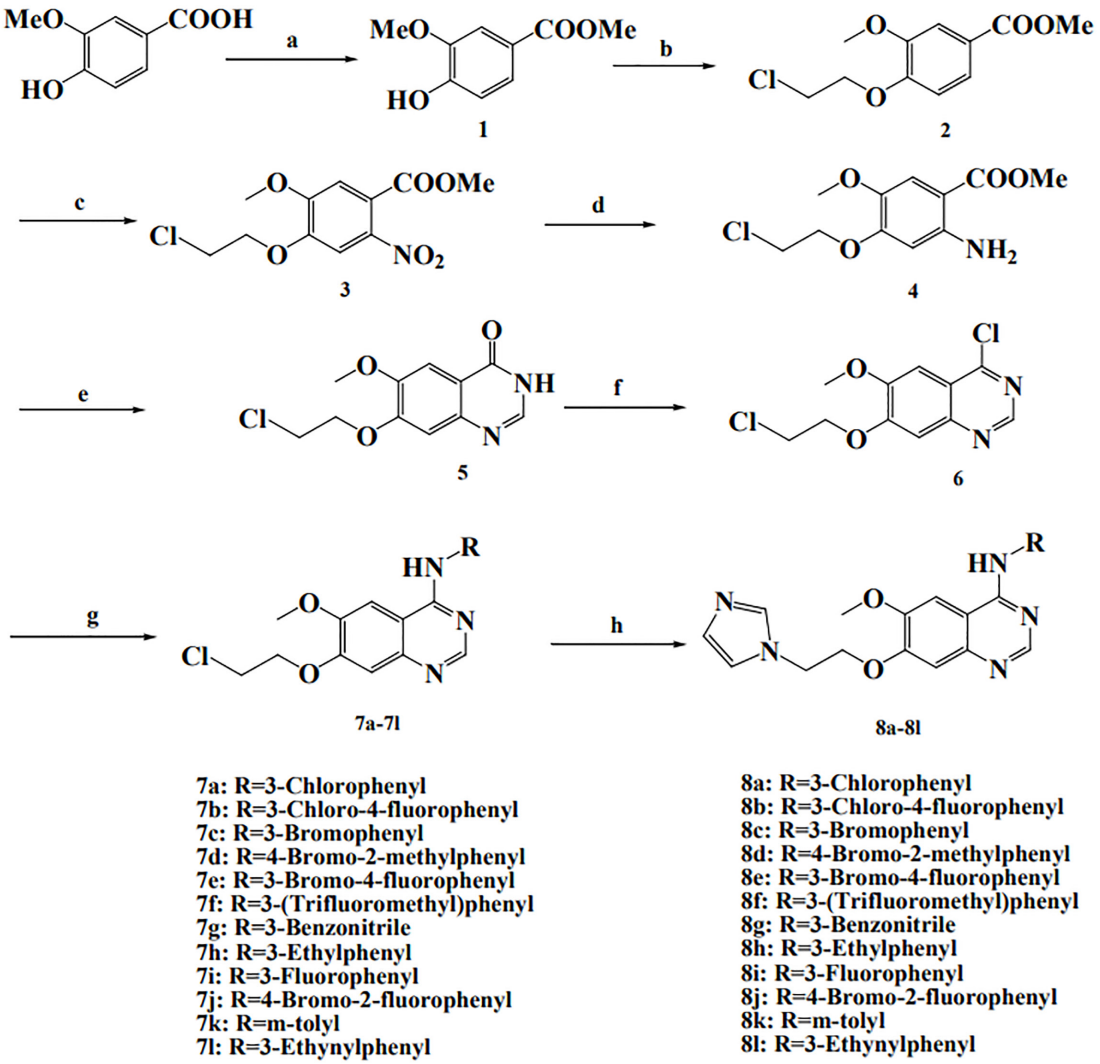

Figure 2. Synthetic pathway of compounds **8a**–**8l**. (a) $SOCl_2$, MeOH, Reflux, 24h; (b) 1-Bromo-2-chloroethane, TBAB, K_2CO_3, Reflux, 4 h; (c) H_2SO_4, HNO_3, 0–5°C, 6h; (d) Fe, NH_4Cl, MeOH/H_2O, Reflux, 4.5 h; (e) formamidine acetate, Ethanol, Reflux, 6 h; (f) Oxalyl chloride, DMF, Dichloromethane, rt, 48 h; (g) Aniline derivatives, i-PrOH, Reflux, 3 h; (h) KI and DMF or choline chloride:urea, Imidazole, Reflux, 2 h.

The yields and reaction time were compared.[43,49,50]
The melting point, IR, ^{1}HNMR, ^{13}CNMR, and elemental analysis data for all these compounds were consistent with previous studies.[7,40] The results for the reaction time and yield of each reaction are presented in Table 1.

Based on results obtained from Table 1, it has been proved that ChCl:urea (1:2) can effectively catalyze the synthesis of compounds **8a-8l**. The proposed mechanism highlights the crucial role played by the ChCl:urea (1:2) (Figure 3).
ChCl:urea (1:2) is capable of forming strong hydrogen bonds, which can create a reactive intermediate. This is followed by a hydrochloric acid abstraction resulting in the formation of the final substitution products. The hypothesis that urea in the DES acts as both a hydrogen-bond donor and acceptor group has been proposed previously.[49,58] Singh and colleagues have reported the synthesis of 2,4-disubstituted quinazolines using DESs. They have demonstrated that DESs, particularly ChCl:urea (1:2), can significantly increase the yield of the ring closure.[59] Also, it has been shown that L-(+)-Tartaric acid and N, N'-Dimethylurea (DMU) as a DES have a significant impact on the yield of quinazolinone synthesis.[60] Similarly, Komar *et al.*[61] have conducted a research on the synthesis of 3-Substituted-quinazolin-4(3H)-ones using ChCl:urea and their results have indicated that DES can be a convenient solvent for this type of the reaction.

The cytotoxicity assessment of the final synthesized agents (**8a-8l)** was carried out on three cell lines, including A431, HUVECs, and HU02, using the MTT assay. As shown in Table 2, out of 12 compounds tested, six compounds demonstrated significant cytotoxic activity against the A431 and HUVEC cell lines. Compounds **8b**, **8c**, **8f**, **8g**, **8k,** and **8l** exhibited higher cytotoxic activity than vandetanib (IC_{50}=10.62 µM) on the A431 cell line, with the IC_{50} values lower than 0.53 µM. Notably, compound **8k** showed the highest cytotoxicity on the A431 cell line with an IC_{50} value of 0.11µM. In a study by Chilin *et al.*,[12] several quinazoline derivatives were synthesized and among them, dioxino 4-anilinoquinazoline bearing 3-methylaniline at position

Table 1. Comparison of yields and time of nucleophilic substitution reactions between 7a-7l and imidazole using potassium iodide/ DMF and ChCl:urea.

Compounds	Potassium iodide and DMF		ChCl:urea (1:2)	
	Time (h)	Yield (%)	Time (min)	Yield (%)
8a	4	42	20	70
8b	4	32	15	62
8c	3.5	40	20	66
8d	4	35	20	65
8e	4	38	15	70
8f	3.5	34	20	60
8g	3.5	30	20	60
8h	4	32	20	63
8i	3.5	35	15	62
8j	4	36	20	60
8k	4	41	15	68
8l	3.5	41	20	72

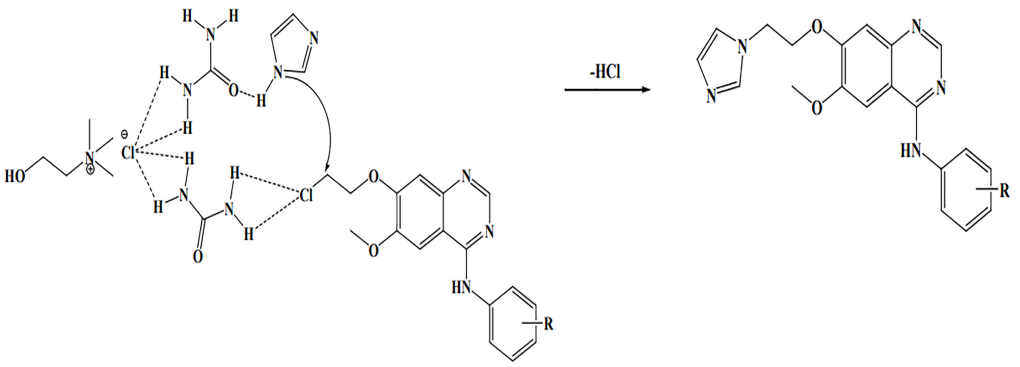

Figure 3. Proposed catalysis mechanism of nucleophilic substitution reaction using ChCl:urea for the synthesis of imidazole-containing quinazoline.

4 of the quinazoline core showed the best cytotoxicity against the A431 cell line with an IC_{50} of 0.67 µM. Another study by Yu *et al.*[14] focused on novel 4-anilinoquinazoline compounds with a 1-adamantyl group at position 4 of the aniline and a methoxyethoxy group at positions 6 and 7 of the quinazoline core, respectively. These compounds demonstrated the best cytotoxicity against the A431 cell line with an IC_{50} of 1.02 µM.Moreover, 6,7-bis(3-morpholinopropoxy)-4-anilinoquinazoline derivatives were prepared and the compound with an (E)-propen-1-yl moiety at position 4 of the aniline showed the best IC_{50} of 1.35 µM.[62] Based on our research and other studies, it appears that lipophilic groups such as methyl, allyl, and halogens on the aniline moiety can enhance cytotoxicity against the A431 cell line.

HUVECs are the most common human endothelial cells, isolated from the endothelium of veins in the umbilical cord. *In vitro* angiogenesis investigations have shown that malignancies with angiogenesis display VEGFR-2 overexpression. It has been established that inhibiting the tyrosine kinase activity of VEGF-induced VEGFR-2 in HUVECs can block the angiogenesis.[63] As is presented in Table 1, most of the synthesized compounds demonstrated moderate to significant cytotoxicity on HUVEC cells. Compounds **8k** and **8l** with *m*-tolyl (**8k**) and 3-ethynyl (**8l**) moieties at the 4-position of the quinazoline scaffold,

Table 2. In vitro antiproliferative activities of compounds 8a–8l on A431, HUVEC, and HU02 cell lines.

Compounds	R	IC_{50}±SD (µM)		
		A431	HUVEC	HU02
	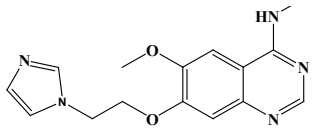			
8a	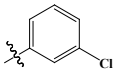	>50	>50	>50
8b	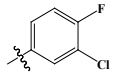	0.1407±0.049	27.15±1.917	>50
8c	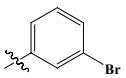	0.4378±0.087	6.92±2.410	6.25
8d	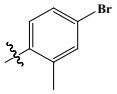	>50	>50	>50
8e	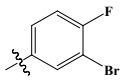	>50	16.52±3.39	>50
8f	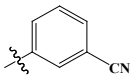	0.5340±0.151	8.107±1.860	>50
8g	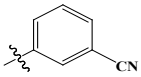	0.3214±0.07	21.91±1.429	>50
8h	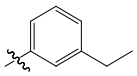	>50	>50	>50
8i	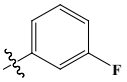	>50	27.29±4.22	>50
8j	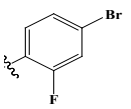	>50	>50	>50
8k	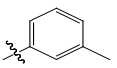	0.1115±0.021	5.017±0.846	12.5
8l	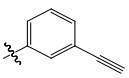	0.2697±0.095	5.243±2.77	>50
Vandetanib		10.62±2.54	5.75±0.84	>50

showed better cytotoxicity (IC_{50} of 5.01 and 5.24 µM, respectively) compared to the reference drug vandetinib (IC_{50}=5.75 µM). Also, compounds **8c** and **8f** exhibited significant cytotoxic activity with IC_{50} values of 6.92 and 8.1 µM against the HUVEC cell line, respectively, which were comparable to vandetanib. Compounds **8b**, **8e**, **8g**, and **8i** also showed noteworthy cytotoxicity on HUVECs (with IC_{50} values of 27.15, 16.52, 21.91, and 27.29 µM, respectively). In a study, urea derivatives of 7-aminoalkoxyquinazoline were synthesized, and most of them showed significant cytotoxicity against the HUVEC cell line with IC_{50} values ranging from 0.12 to 4.39 µM.[64] Elsayed *et al.*[65] reported the cytotoxic activity of some 5-anilinoquinazoline-8-nitro derivatives, showing that compounds with 3-methyl, 2-chloro-5-fluoro, and 2,5-dichloro substituents on phenylurea at the position 4 of the quinazoline scaffold represented significant cytotoxic activity (IC_{50} values of 6.4, 5.7, and 1.8 µM, respectively). A quinazoline with an indazole moiety containing 3,4-dichlorophenyl also showed great potency against the HUVEC cell line (IC_{50} of 0.087 µM). Similar to the results from the A431 cell line, the aniline group with lipophilic substituents showed more cytotoxic activity on the HUVEC cell line.[22] Compounds **8k** and **8l** showed significantly greater cytotoxicity than the positive control on both A431 and HUVEC cell lines (IC_{50} values of 0.11 µM and 0.26 µM against A431 and 5.01 and 5.24µM on HUVECs, respectively). These compounds likely exhibit significant cytotoxic effects by blocking the EGFR and VEGFR-2 tyrosine kinase activities, making them promising candidates for further studies in developing new anticancer agents. It is worth noting that most of the compounds revealed no cytotoxicity against the HU02 healthy cell line (IC_{50}>50 µM), except for compounds **8c** and **8k,** which had IC_{50} values of 6.25 and 12.5 µM. This may be due to the normal expression of EGFR and VEGFR-2 in this cell line. Given the potent cytotoxic effect of compound **8l** on A431 and HUVEC cell lines, without showing any cytotoxicity on the HU02 cell line, it is more likely that this compound exerts its effect through the inhibition of tyrosine kinase activity of EGFR and VEGFR-2. Further investigation of the inhibitory activity of potent compounds on EGFR and VEGFR-2 tyrosine kinase is suggested to determine their exact mechanism of action.

Furthermore, to explore the interaction of the most potent synthesized compound **8k** and vandetanib (the standard drug), molecular docking investigations were conducted into the ATP binding site of EGFR (PDB ID: 1M17) and VEGFR-2 (PDB ID: 2RL5) using AutoDock 4.2 and AutoDock Tools 1.5.4 (ADT).[54] The validation was carried out by the active conformation of the ligand co-crystal structures.

Figure 4 illustrates that the quinazoline N1 of compound **8k** and vandetanib form hydrogen bonds with **Met769** of the EGFR ATP-binding site with docking scores of -8.76 and -8.02 kcal/mol, respectively (8k: 1.928 Å , vandetanib: 1.638 Å). This bond is crucial for the proper fitting of the quinazoline scaffold in the EGFR binding site. Also, hydrophobic interactions were observed between both compounds and residues in the hydrophobic pocket of the EGFR active site. These residues include **Val702, Ala719, Lys721, Met742, Leu764,** and **Thr766** for compound **8k** and **Val702, Ala719, Lys721, Glu738, Met742,** and **Leu764** for vandetanib (Figure 4). Different studies have reported similar interactions between EGFR tyrosine kinase inhibitors and the ATP-binding site of EGFR tyrosine kinase. In all of these studies, the hydrogen bond interaction between the heterocyclic nitrogen and **Met769** of EGFR, which is a key residue, was found to be the most important bond for the optimal fitting of inhibitors in the active site. Furthermore, hydrophobic interactions with **Leu694** and **Leu820,** as well as π-cation interaction with **Lys721,** have been reported. The quinazoline core also exhibited hydrophobic interactions with **Ile765**, **Ala719**, **Met769**, **Leu694**, and **Leu768** amino acids. It is worth mentioning that the substituted aniline ring displayed

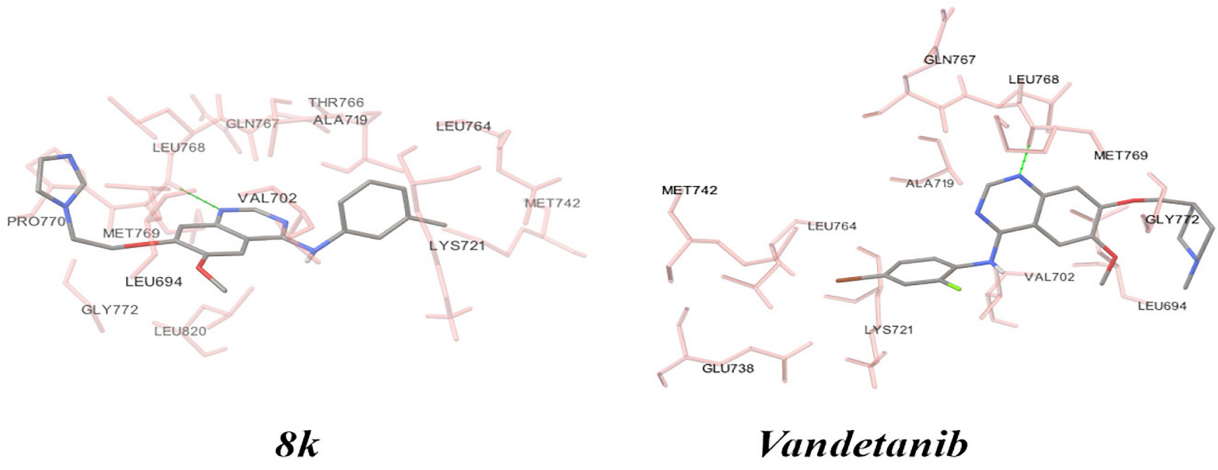

Figure 4. Docking interactions of compound **8k** and vandetanib with EGFR.

hydrophobic interactions with **Phe832**, **Leu764**, **Leu753**, **Met742**, **Ile720,** and **Ile765** as well as polar interactions with **Thr830** and **Thr766** residues.[66-71]

Moreover, the interaction study of compound **8k** and vandetanib with the VEGFR-2 ATP-binding site showed the formation of one hydrogen bond. This bond occurred between the imidazole-N3 of **8k** and the aquinazoline-N1of vandetanib, as well as **Cys919** of the active site of VEGFR-2 (**8k**: -9.03kcal/mol, 2.81 Å; Vandetanib: -8.97kcal/mol, 2.12 Å). The m-tolyl of compound **8k** formed hydrophobic interactions with a hydrophobic pocket created by **Val848, Ala866, Lys868, Thr916,** and **Phe1047.** On the other hand, the 4-bromo-2-fluoroaniline of vandetanib interacted with **Cys1045**, **Asp1046,** and **Phe1047** (Figure 5). In line with other studies, the **Cys919** residue formed a critical hydrogen bond with nitrogen of the different heterocyclic rings, such as quinazoline, pyrimidine, indole, and quinolone. Also, the inhibitors showed other interactions, including π–π stacking interaction with **Phe1047**, π–cation interaction with **Lys868**, and π–alkyl interactions with different residues, such as **Leu840**, **Leu1035**, **Val916**, **Val848**, **Ala866**, **Ile888**, **Leu889**, **Val899**, **Phe918**, **Thr916**, and **Cys1045.**[72-74]

Because of the undeniable role of cell migration in cancer development and metastasis, a cell migration assay was performed to study the impact of compounds **8b**, **8c**, **8e**, **8f**, **8g**, **8i**, **8k,** and **8l** on the cell migration of the HUVECs. The investigation results demonstrated that all tested compounds were able to block the process of cell migration. As shown in Figure 6, the cells were treated with 10 µM of each compound for 24 h. After this time, the wound closure percentages were 15%, 50%, 40%, 30%, 18%, 9%, and 12% for compounds **8b, 8c, 8e, 8f, 8g, 8i, 8k, and 8l**, respectively. Compared to the control group, which had no inhibition and achieved 100% wound closure, all of the above compounds represented significant inhibitory effects on cell migration. Compounds **8k** and **8l** displayed higher potency than the other examined compounds. The synthesis of quinazoline-4(3H)-ones and sulfachloropyridazine derivatives showed that the compound with a phenethyl group at the position 3 of the quinazoline had a wound closure of 58.52% at a concentration of 10 µg/mL after 72 h, compared to the control group with 99% wound closure.[75] Also, benzoxazole derivatives synthesized by Elkady *et al.*[76] represented a significant decrease in wound closure in the compound with methoxy and chloro groups (47.2% ± 2.88) in comparison with the control group (95.86 %± 4.51).

Conclusion

To summarize, a series of 4-anilinoquinazoline derivatives were designed and synthesized as cytotoxic agents, with various substitutions at the C-7 position of the quinazoline core. These compounds were tested on two cancer cell lines (A431 and HUVEC) as well as one healthy cell line (HU02). The results indicated that the use of DES significantly improved the yield and decreased the reaction time. Most of the synthesized compounds demonstrated significant cytotoxic activity on cancer cell lines, while showing no apparent cytotoxicity to HU02. Notably, compound **8k** exhibited the highest cytotoxicity on both cancer cell lines. Molecular docking studies confirmed that compound **8k** had a higher binding affinity to both EGFR and VEGFR-2 compared to vandetanib. Furthermore, compound **8k** showed the strongest inhibitory activity on cell migration. These findings suggest that compound **8k** could be a promising candidate for further study and structural optimization as an anticancer agent.

Ethical Issues

This study was approved by the Ethical Committee of

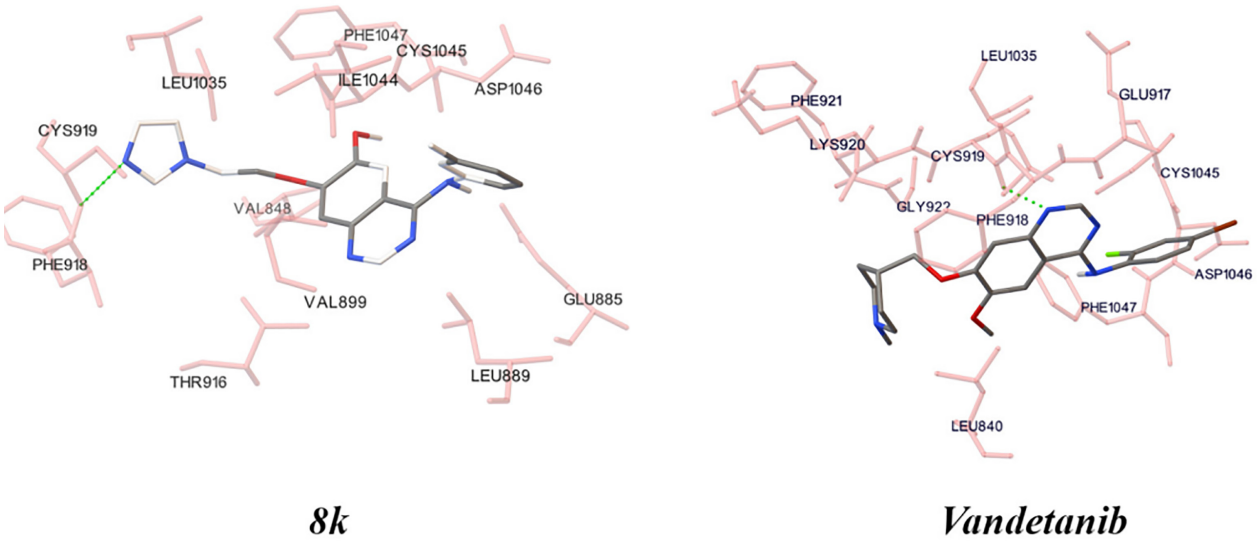

Figure 5. Docking interactions of compound **8k** and vandetanib with VEGFR-2.

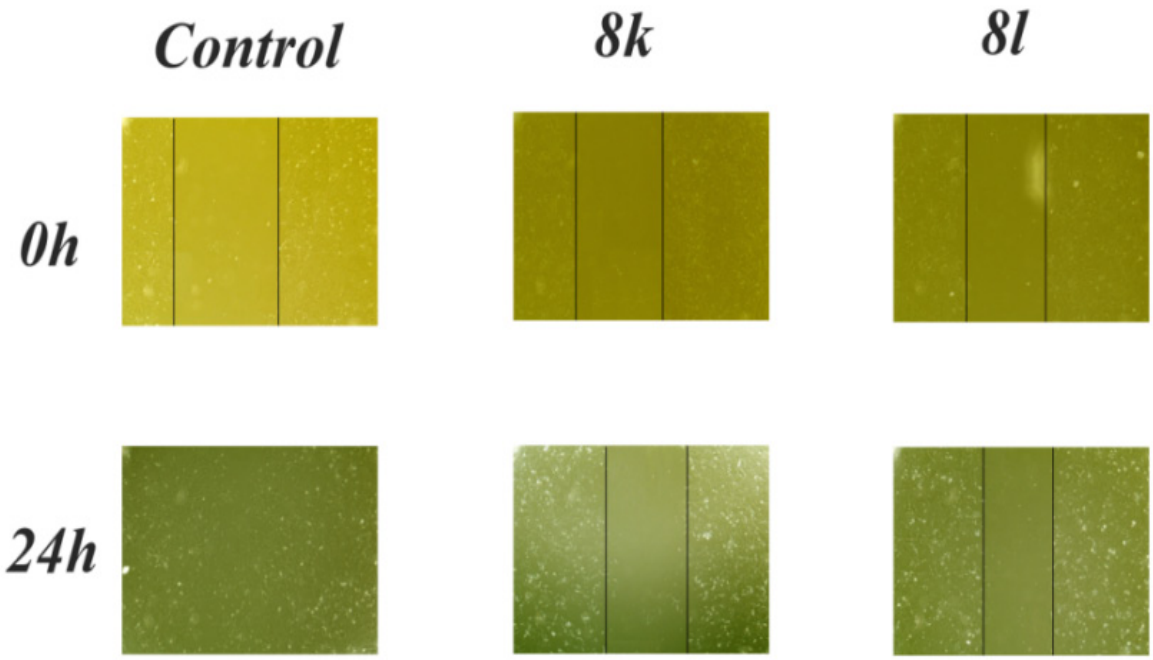

Figure 6. Effect of compounds **8k** and **8l** on cell migration of HUVEC cells at 0 and 24 h using wound-healing assay.

Guilan University of Medical Sciences (ID: IR. GUMS. REC. 1398. 219, Date: 3.August.2019).

Acknowledgments

This work was supported by Guilan University of Medical Sciences.

Author Contributions

Fatemeh Azmian Moghadam: Methodology, Investigation, Formal Analysis. Sara Dabirian: Investigation, Formal Analysis. Amin Ebrahimi Tavani: Investigation, Formal Analysis. Parisa Alipour: Investigation, Formal Analysis. Mohammad Mojabi: Investigation, Formal Analysis. Mehdi Evazalipour: Formal Analysis. Fatemeh Yousefbeyk: Investigation, Formal Analysis, Writing - Review & Editing. Saeed Ghasemi: Supervision, Conceptualization, Investigation, Formal Analysis, Writing - Original Draft.

Conflict of Interest

The authors confirm that this article's content has no conflicts of interest.

References

1. Alkamaly OM, Altwaijry N, Sabour R, Harras MF. Dual EGFR/VEGFR2 inhibitors and apoptosis inducers: Synthesis and antitumor activity of novel pyrazoline derivatives. Arch Pharm. 2021;354(4):2000351. doi:10.1002/ardp.202000351
2. World Health Organization, https://www.who.int. Available from: https://www.who.int/news-room/fact-sheets/detail/cancer
3. Holohan C, Van Schaeybroeck S, Longley DB, Johnston PG. Cancer drug resistance: An evolving paradigm. Nat Rev Cancer. 2013;13(10):714-26. doi:10.1038/nrc3599
4. Agarwal E, Brattain MG, Chowdhury S. Cell survival and metastasis regulation by akt signaling in colorectal cancer. Cell Signal. 2013;25(8):1711-9. doi:10.1016/j.cellsig.2013.03.025
5. Lemmon MA, Schlessinger J. Cell signaling by receptor tyrosine kinases. Cell. 2010;141(7):1117-34. doi:10.1016/j.cell.2010.06.011
6. Liao JJ-L. Molecular recognition of protein kinase binding pockets for design of potent and selective kinase inhibitors. J Med Chem. 2007;50(3):409-24. doi:10.1021/jm0608107
7. Moghadam FA, Dabirian S, Dogaheh MG, Mojabi M, Yousefbeyk F, Ghasemi S. Novel 4-anilinoquinazoline derivatives as potent anticancer agents: Design, synthesis, cytotoxic activity, and docking study. Aust J Chem. 2021;74(10):730-9. doi:10.1071/CH21147
8. Sheng Q, Liu J. The therapeutic potential of targeting the egfr family in epithelial ovarian cancer. Br J Cancer. 2011;104(8):1241-5. doi:10.1038/bjc.2011.62
9. Janmaat ML, Giaccone G. Small-molecule epidermal growth factor receptor tyrosine kinase inhibitors. Oncologist. 2003;8(6):576-86. doi:10.1634/theoncologist.8-6-576
10. de Castro Barbosa ML, Lima LM, Tesch R, Sant'Anna CMR, Totzke F, Kubbutat MH, et al. Novel 2-chloro-4-anilino-quinazoline derivatives as egfr and vegfr-2 dual inhibitors. Eur J Med Chem. 2014;71:1-14. doi:10.1016/j.ejmech.2013.10.058
11. El-Naggar AM, Hassan A, Elkaeed EB, Alesawy MS, Al-Karmalawy AA. Design, synthesis, and sar studies of novel 4-methoxyphenyl pyrazole and pyrimidine

derivatives as potential dual tyrosine kinase inhibitors targeting both egfr and vegfr-2. Bioorg Chem. 2022;123:105770. doi:10.1016/j.bioorg.2022.105770
12. Chilin A, Conconi MT, Marzaro G, Guiotto A, Urbani L, Tonus F, et al. Exploring epidermal growth factor receptor (egfr) inhibitor features: The role of fused dioxygenated rings on the quinazoline scaffold. J Med Chem. 2010;53(4):1862-6. doi:10.1021/jm901338g
13. Pawar VG, Sos ML, Rode HB, Rabiller M, Heynck S, Van Otterlo WA, et al. Synthesis and biological evaluation of 4-anilinoquinolines as potent inhibitors of epidermal growth factor receptor. J Med Chem. 2010;53(7):2892-901. doi:10.1021/jm901877j
14. Yu H, Li Y, Ge Y, Song Z, Wang C, Huang S, et al. Novel 4-anilinoquinazoline derivatives featuring an 1-adamantyl moiety as potent egfr inhibitors with enhanced activity against nsclc cell lines. Eur J Med Chem. 2016;110:195-203. doi:10.1016/j.ejmech.2016.01.045
15. Kim Y-s, Li F, O'Neill BE, Li Z. Specific binding of modified zd6474 (vandetanib) monomer and its dimer with vegf receptor-2. Bioconjug Chem. 2013;24(11):1937-44. doi:10.1021/bc400374t
16. Nishida N, Yano H, Nishida T, Kamura T, Kojiro M. Angiogenesis in cancer. Vasc Health Risk Manag. 2006;2(3):213. doi:10.2147/vhrm.2006.2.3.213
17. Shi L, Wu T-T, Wang Z, Xue J-Y, Xu Y-G. Discovery of quinazolin-4-amines bearing benzimidazole fragments as dual inhibitors of c-met and vegfr-2. Bioorg Med Chem. 2014;22(17):4735-44. doi:10.1016/j.bmc.2014.07.008
18. Wang X, Bove AM, Simone G, Ma B. Molecular bases of vegfr-2-mediated physiological function and pathological role. Front Cell Dev Biol. 2020;8:1314. doi:10.3389/fcell.2020.599281
19. Hasegawa M, Nishigaki N, Washio Y, Kano K, Harris PA, Sato H, et al. Discovery of novel benzimidazoles as potent inhibitors of tie-2 and vegfr-2 tyrosine kinase receptors. J Med Chem. 2007;50(18):4453-70. doi:10.1021/jm0611051
20. Garofalo A, Goossens L, Lemoine A, Farce A, Arlot Y, Depreux P. Quinazoline-urea, new protein kinase inhibitors in treatment of prostate cancer. J Enzyme Inhib Med Chem. 2010;25(2):158-71. doi:10.3109/14756360903169485
21. Wissner A, Fraser HL, Ingalls CL, Dushin RG, Floyd MB, Cheung K, et al. Dual irreversible kinase inhibitors: Quinazoline-based inhibitors incorporating two independent reactive centers with each targeting different cysteine residues in the kinase domains of egfr and vegfr-2. Bioorg Med Chem. 2007;15(11):3635-48. doi:10.1016/j.bmc.2007.03.055
22. Xi L, Zhang J-Q, Liu Z-C, Zhang J-H, Yan J-F, Jin Y, et al. Novel 5-anilinoquinazoline-8-nitro derivatives as inhibitors of VEGFR-2 tyrosine kinase: Synthesis, biological evaluation and molecular docking. Org Biomol Chem. 2013;11(26):4367-78. doi:10.1039/C3OB40368H
23. Garofalo A, Goossens L, Lemoine A, Ravez S, Six P, Howsam M, et al. [4-(6, 7-disubstituted quinazolin-4-ylamino) phenyl] carbamic acid esters: A novel series of dual egfr/vegfr-2 tyrosine kinase inhibitors. Medchemcomm. 2011;2(1):65-72. doi:10.1039/C0MD00183J
24. Garofalo A, Goossens L, Six P, Lemoine A, Ravez S, Farce A, et al. Impact of aryloxy-linked quinazolines: A novel series of selective vegfr-2 receptor tyrosine kinase inhibitors. Bioorg Med Chem Lett. 2011;21(7):2106-12. doi:10.1016/j.bmcl.2011.01.137
25. Xu P, Chu J, Li Y, Wang Y, He Y, Qi C, et al. Novel promising 4-anilinoquinazoline-based derivatives as multi-target rtks inhibitors: Design, molecular docking, synthesis, and antitumor activities in vitro and vivo. Bioorg Med Chem. 2019;27(20):114938. doi:10.1016/j.bmc.2019.06.001
26. Ismail RS, Abou-Seri SM, Eldehna WM, Ismail NS, Elgazwi SM, Ghabbour HA, et al. Novel series of 6-(2-substitutedacetamido)-4-anilinoquinazolines as egfr-erk signal transduction inhibitors in mcf-7 breast cancer cells. Eur J Med Chem. 2018;155:782-96. doi:10.1016/j.ejmech.2018.06.024
27. Wei H, Duan Y, Gou W, Cui J, Ning H, Li D, et al. Design, synthesis and biological evaluation of novel 4-anilinoquinazoline derivatives as hypoxia-selective egfr and vegfr-2 dual inhibitors. Eur J Med Chem. 2019;181:111552. doi:10.1016/j.ejmech.2019.07.055
28. Hennequin LF, Stokes ES, Thomas AP, Johnstone C, Plé PA, Ogilvie DJ, et al. Novel 4-anilinoquinazolines with c-7 basic side chains: Design and structure activity relationship of a series of potent, orally active, vegf receptor tyrosine kinase inhibitors. J Med Chem. 2002;45(6):1300-12. doi:10.1021/jm011022e
29. Hennequin LF, Thomas AP, Johnstone C, Stokes ES, Plé PA, Lohmann J-JM, et al. Design and structure–activity relationship of a new class of potent vegf receptor tyrosine kinase inhibitors. J Med Chem. 1999;42(26):5369-89. doi:10.1021/jm990345w
30. Zhang H-Q, Gong F-H, Li C-G, Zhang C, Wang Y-J, Xu Y-G, et al. Design and discovery of 4-anilinoquinazoline-acylamino derivatives as egfr and vegfr-2 dual tk inhibitors. Eur J Med Chem. 2016;109:371-9. doi:10.1016/j.ejmech.2015.12.032
31. Zhang Q, Vigier KDO, Royer S, Jérôme F. Deep eutectic solvents: Syntheses, properties and applications. Chem Soc Rev. 2012;41(21):7108-46. doi:10.1039/C2CS35178A
32. Khandelwal S, Tailor YK, Kumar M. Deep eutectic solvents (DESs) as eco-friendly and sustainable solvent/catalyst systems in organic transformations. J Mol Liq. 2016;215:345-86. doi:10.1016/j.molliq.2015.12.015
33. Abbott AP, Capper G, Davies DL, Rasheed RK, Tambyrajah V. Novel solvent properties of choline chloride/urea mixtures. Chem Commun. 2003;7:70-1. doi:10.1039/B210714G

34. Azizi N, Alipour M. Eco-efficiency and scalable synthesis of bisamides in deep eutectic solvent. J Mol Liq. 2015;206:268-71. doi:10.1016/j.molliq.2015.02.033
35. Azizi N, Ahooie TS, Hashemi MM. Multicomponent domino reactions in deep eutectic solvent: An efficient strategy to synthesize multisubstituted cyclohexa-1, 3-dienamines. J Mol Liq. 2017;246:221-4. doi:10.1016/j.molliq.2017.09.049
36. Cecone C, Hoti G, Bracco P, Trotta F. Natural deep eutectic solvents (NADES)- progress in polymer synthesis and pharmaceutical application. Pharm Sci. 2022;28(4):492-5. doi:10.34172/ps.2022.31
37. Abtahi B, Tavakol H. Choline chloride-urea deep eutectic solvent as an efficient media for the synthesis of propargylamines via organocuprate intermediate. Appl Organometal Chem. 2020;34(11):e5895. doi:10.1002/aoc.5895
38. Amoroso R, Hollmann F, Maccallini C. Choline chloride-based DES as solvents/catalysts/chemical donors in pharmaceutical synthesis. Molecules. 2021;26(20):6286. doi:10.3390/molecules26206286
39. Sharma P, LaRosa C, Antwi J, Govindarajan R, Werbovetz KA. Imidazoles as potential anticancer agents: An update on recent studies. Molecules. 2021;26(14):4213. doi:10.3390/molecules26144213
40. Moghadam FA, Evazalipour M, Kefayati H, Ghasemi S. 6, 7-disubstituted-4-anilinoquinazoline: Design, synthesis and anticancer activity as a novel series of potent anticancer agents. Pharm Sci. 2021;27(2):209-18. doi:10.34172/PS.2020.72
41. Azmian Moghadam F, Evazalipour M, Ghasemi S, Kefayati H. Design, synthesis, biological evaluation and docking study of novel 4-anilinoquinazolines derivatives as anticancer agents. Iran J Chem Chem Eng. 2022;41(2):353-67. doi:10.30492/IJCCE.2020.132389.4271
42. Li R-D, Zhang X, Li Q-Y, Ge Z-M, Li R-T. Novel egfr inhibitors prepared by combination of dithiocarbamic acid esters and 4-anilinoquinazolines. Bioorg Med Chem Lett. 2011;21(12):3637-40. doi:10.1016/j.bmcl.2011.04.096
43. Zhao F, Lin Z, Wang F, Zhao W, Dong X. Four-membered heterocycles-containing 4-anilino-quinazoline derivatives as epidermal growth factor receptor (EGFR) kinase inhibitors. Bioorg Med Chem Lett. 2013;23(19):5385-8. doi:10.1016/j.bmcl.2013.07.049
44. Ghasemi S, Sharifi S, Mojarrad JS. Design, synthesis and biological evaluation of novel piperazinone derivatives as cytotoxic agents. Adv Pharm Bull. 2020;10(3):423. doi:10.34172/apb.2020.051
45. Holladay MW, Campbell BT, Rowbottom MW, Chao Q, Sprankle KG, Lai AG, et al. 4-quinazolinyloxy-diaryl ureas as novel brafv600e inhibitors. Bioorg Med Chem Lett. 2011;21(18):5342-6. doi:10.1016/j.bmcl.2011.07.019
46. Mozaffari S, Ghasemi S, Baher H, Khademi H, Amini M, Sakhteman A, et al. Synthesis and evaluation of some novel methylene-bridged aryl semicarbazones as potential anticonvulsant agents. Med Chem Res. 2012;21(11):3797-808. doi:10.1007/s00044-011-9924-6
47. Zhang N, Wu B, Powell D, Wissner A, Floyd MB, Kovacs ED, et al. Synthesis and structure–activity relationships of 3-cyano-4-(phenoxyanilino) quinolines as mek (mapkk) inhibitors. Bioorg Med Chem Lett. 2000;10(24):2825-8. doi:10.1016/S0960-894X(00)00580-1
48. Mojarrad JS, Zamani Z, Nazemiyeh H, Ghasemi S, Asgari D. Synthesis of novel 1, 4-dihydropyridine derivatives bearing biphenyl-2'-tetrazole substitution as potential dual angiotensin ii receptors and calcium channel blockers. Adv Pharm Bull. 2011;1(1):1. doi:10.5681/apb.2011.001
49. Yadav UN, Shankarling GS. Synergistic effect of ultrasound and deep eutectic solvent choline chloride–urea as versatile catalyst for rapid synthesis of β-functionalized ketonic derivatives. J Mol Liq. 2014;195:188-93. doi:10.1016/j.molliq.2014.02.016
50. Garofalo A, Farce A, Ravez Sv, Lemoine Al, Six P, Chavatte P, et al. Synthesis and structure–activity relationships of (aryloxy) quinazoline ureas as novel, potent, and selective vascular endothelial growth factor receptor-2 inhibitors. J Med Chem. 2012;55(3):1189-204. doi:10.1021/jm2013453
51. Shi Y, Gao Q, Chen X, Mi Y, Zhang Y, Yang H, et al. WIPO patent. WO2016023330. 2016.
52. Hamidi M, Ghasemi S, Bavafa Bighdilou B, Eghbali Koohi D. Evaluation of antioxidant, antibacterial and cytotoxic activity of methanol extract from leaves and fruits of iranian squirting cucumber (*Ecballium elaterium* (L.) a. Rich). Res J Pharmacogn. 2020;7(1):23-9. doi:10.22127/rjp.2019.190800.1509
53. Ghasemi S, Davaran S, Sharifi S, Abdollahi A, Mojarrad JS. Comparison of cytotoxic activity of l778123 as a farnesyltranferase inhibitor and doxorubicin against a549 and ht-29 cell lines. Adv Pharm Bull. 2013;3(1):73. doi:10.5681/apb.2013.012
54. Robichaux JP, Elamin YY, Tan Z, Carter BW, Zhang S, Liu S, et al. Mechanisms and clinical activity of an egfr and her2 exon 20–selective kinase inhibitor in non–small cell lung cancer. Nat Med. 2018;24(5):638-46. doi:10.1038/s41591-018-0007-9
55. Cheng W-Y, Chiao M-T, Liang Y-J, Yang Y-C, Shen C-C, Yang C-Y. Luteolin inhibits migration of human glioblastoma u-87 mg and t98g cells through downregulation of cdc42 expression and pi3k/akt activity. Mol Biol Rep. 2013;40(9):5315-26. doi:10.1007/s11033-013-2632-1
56. Shen F-Q, Shi L, Wang Z-F, Wang C-R, Chen J-J, Liu Y, et al. Design, synthesis, biological evaluation of benzoyl amide derivatives containing nitrogen heterocyclic ring as potential vegfr-2 inhibitors. Bioorg Med Chem.

2019;27(17):3813-24. doi:10.1016/j.bmc.2019.07.007
57. Zhang Y, Gao H, Liu R, Liu J, Chen L, Li X, et al. Quinazoline-1-deoxynojirimycin hybrids as high active dual inhibitors of egfr and α-glucosidase. Bioorg Med Chem Lett. 2017;27(18):4309-13. doi:10.1016/j.bmcl.2017.08.035
58. Hawkins I, Handy ST. Synthesis of aurones under neutral conditions using a deep eutectic solvent. Tetrahedron. 2013;69(44):9200-4. doi: 10.1016/j.tet.2013.08.060
59. Singh RR, Singh TP, Devi TL, Devi TJ, Singh OM. Synthesis of 2, 4-disubstituted quinazolines promoted by deep eutectic solvent. Curr Opin Green Sustain Chem. 2021;4:100130. doi:10.1016/j.crgsc.2021.100130
60. Ghosh SK, Nagarajan R. Deep eutectic solvent mediated synthesis of quinazolinones and dihydroquinazolinones: Synthesis of natural products and drugs. RSC Adv. 2016;6(33):27378-87. doi:10.1039/C6RA00855K
61. Komar M, Molnar M, Jukić M, Glavaš-Obrovac L, Opačak-Bernardi T. Green chemistry approach to the synthesis of 3-substituted-quinazolin-4 (3 h)-ones and 2-methyl-3-substituted-quinazolin-4 (3 h)-ones and biological evaluation. Green Chem Lett Rev. 2020;13(2):93-101. doi:10.1080/17518253.2020.1741694
62. Chen L, Zhang Y, Liu J, Wang W, Li X, Zhao L, et al. Novel 4-arylaminoquinazoline derivatives with (e)-propen-1-yl moiety as potent EGFR inhibitors with enhanced antiproliferative activities against tumor cells. Eur J Med Chem. 2017;138:689-97. doi:10.1016/j.ejmech.2017.06.023
63. Zhang Y, Chen Y, Zhang D, Wang L, Lu T, Jiao Y. Discovery of novel potent VEGFR-2 inhibitors exerting significant antiproliferative activity against cancer cell lines. J Med Chem. 2018;61(1):140-57. doi:10.1021/acs.jmedchem.7b01091
64. Ravez S, Barczyk A, Six P, Cagnon A, Garofalo A, Goossens L, et al. Inhibition of tumor cell growth and angiogenesis by 7-aminoalkoxy-4-aryloxy-quinazoline ureas, a novel series of multi-tyrosine kinase inhibitors. Eur J Med Chem. 2014;79:369-81. doi:10.1016/j.ejmech.2014.04.007
65. Elsayed NM, Serya RA, Tolba MF, Ahmed M, Barakat K, Abou El Ella DA, et al. Design, synthesis, biological evaluation and dynamics simulation of indazole derivatives with antiangiogenic and antiproliferative anticancer activity. Bioorg Chem. 2019;82:340-59. doi:10.1016/j.bioorg.2018.10.071
66. Sangande F, Julianti E, Tjahjono DH. Ligand-based pharmacophore modeling, molecular docking, and molecular dynamic studies of dual tyrosine kinase inhibitor of egfr and VEGFR2. Int J Mol Sci. 2020;21(20):7779. doi:10.3390/ijms21207779
67. Nasab RR, Mansourian M, Hassanzadeh F, Shahlaei M. Exploring the interaction between epidermal growth factor receptor tyrosine kinase and some of the synthesized inhibitors using combination of in-silico and in-vitro cytotoxicity methods. Res Pharm Sci. 2018;13(6):509. doi:10.4103/1735-5362.245963
68. Al-Warhi T, El Kerdawy AM, Said MA, Albohy A, Elsayed ZM, Aljaeed N, et al. Novel 2-(5-aryl-4, 5-dihydropyrazol-1-yl) thiazol-4-one as egfr inhibitors: Synthesis, biological assessment and molecular docking insights. Drug Des Devel Ther. 2022;16:1457-71. doi:10.2147/DDDT.S356988
69. Verma G, Khan MF, Akhtar W, Alam MM, Akhter M, Alam O, et al. Pharmacophore modeling, 3d-qsar, docking and adme prediction of quinazoline based egfr inhibitors. Arab J Chem. 2019;12(8):4815-39. doi:10.1016/j.arabjc.2016.09.019
70. Thirumurugan K, Lakshmanan S, Govindaraj D, Daniel Prabu DS, Ramalakshmi N, Arul Antony S. Design, synthesis and anti-inflammatory activity of pyrimidine scaffold benzamide derivatives as epidermal growth factor receptor tyrosine kinase inhibitors. J Mol Struct. 2018;1171:541-50. doi:10.1016/j.molstruc.2018.06.003
71. Choowongkomon K, Sawatdichaikul O, Songtawee N, Limtrakul J. Receptor-based virtual screening of egfr kinase inhibitors from the nci diversity database. Molecules. 2010;15(6):4041-54. doi:10.3390/molecules15064041
72. Meng F. Molecular dynamics simulation of VEGFR2 with sorafenib and other urea-substituted aryloxy compounds. J Theor Chem. 2013;2013:739574. doi:10.1155/2013/739574
73. Marzouk AA, Abdel-Aziz SA, Abdelrahman KS, Wanas AS, Gouda AM, Youssif BG, et al. Design and synthesis of new 1, 6-dihydropyrimidin-2-thio derivatives targeting vegfr-2: Molecular docking and antiproliferative evaluation. Bioorg Chem. 2020;102:104090. doi:10.1016/j.bioorg.2020.104090
74. Kang D, Pang X, Lian W, Xu L, Wang J, Jia H, et al. Discovery of vegfr2 inhibitors by integrating naïve bayesian classification, molecular docking and drug screening approaches. RSC Adv. 2018;8(10):5286-97. doi:10.1039/C7RA12259D
75. Zahran SS, Ragab FA, El-Gazzar MG, Soliman AM, Mahmoud WR, Ghorab MM. Antiproliferative, antiangiogenic and apoptotic effect of new hybrids of quinazoline-4 (3h)-ones and sulfachloropyridazine. Eur J Med Chem. 2023;245:114912. doi:10.1016/j.ejmech.2022.114912
76. Elkady H, Elwan A, El-Mahdy HA, Doghish AS, Ismail A, Taghour MS, et al. New benzoxazole derivatives as potential vegfr-2 inhibitors and apoptosis inducers: Design, synthesis, anti-proliferative evaluation, flowcytometric analysis, and in silico studies. J Enzyme Inhib Med Chem. 2022;37(1):403-16. doi:10.1080/14756366.2021.2015343